Published as: *Geobiology*. 2007 June ; 5(2): 119–126.

A likely role for anoxygenic photosynthetic microbes in the formation of ancient stromatolites

T. Bosak[1,*], **S. E. Greene**[1], and **D. K. Newman**[1,2,3]

[1]Division of Geological and Planetary Sciences, California Institute of Technology, Pasadena, USA

[2]Division of Biology, California Institute of Technology, Pasadena, USA

[3]Howard Hughes Medical Institute, California Institute of Technology, Pasadena, USA

Abstract

Although cyanobacteria are the dominant primary producers in modern stromatolites and other microbialites, the oldest stromatolites pre-date geochemical evidence for oxygenic photosynthesis and cyanobacteria in the rock record. As a step towards the development of laboratory models of stromatolite growth, we tested the potential of a metabolically ancient anoxygenic photosynthetic bacterium to build stromatolites. This organism, *Rhodopseudomonas palustris*, stimulates the precipitation of calcite in solutions already highly saturated with respect to calcium carbonate, and greatly facilitates the incorporation of carbonate grains into proto-lamina (i.e. crusts). The appreciable stimulation of the growth of proto-lamina by a nonfilamentous anoxygenic microbe suggests that similar microbes may have played a greater role in the formation of Archean stromatolites than previously assumed.

INTRODUCTION

A stromatolite is ‘an attached, laminated, lithified sedimentary growth structure accretionary away from a point or a limited surface of initiation’ (Semikhatov *et al.*, 1979). These rocks have a sedimentary record more than 3 billion years long, and, although the definition of a stromatolite above does not imply a biogenic origin, the oldest putative macrofossils are, in fact, stromatolites (Walter *et al.*, 1980; Hoffman H.J., 1999).

When the biogenicity of Archean stromatolites is not disputed (Buick *et al.*, 1981; Lowe, 1994; Buick *et al.*, 1995; Grotzinger & Rothman, 1996), it is often assumed that they reflect the presence of oxygenic phototrophs (see Altermann *et al.*, 2006 for a review). Cyanobacterial photosynthesis drives the microbial communities intimately associated with modern marine stromatolites, hypersaline stromatolites and stromatolites that form in alkaline lakes (Riding *et al.*, 1991; Reid *et al.*, 2000; Kazmierczak & Kempe, 2006), but most would agree that there is no compelling evidence for widespread oxygenic photosynthesis (Dietrich *et al.*, 2006) at the time when the first extensive Archean stromatolitic reefs formed (Allwood *et al.*, 2006). This prompts us to consider the roles of other organisms with O_2-independent metabolisms in stromatolite formation.

Anoxygenic photosynthesis could have driven primary production in shallow marine environments before the rise of oxygenic photosynthesis and the widespread atmospheric

Corresponding author: D. K. Newman. Tel.: 1 626 395 6790; fax: 1 626 688 0621; dkn@gps.caltech.edu.
*Present address: Department of Molecular and Cellular Biology, Harvard University, Cambridge, MA 02138, USA.

oxygenation (Olson & Blankenship, 2004). Consequently, some Archean stromatolites may have hosted microbial communities that were not driven by oxygenic photosynthesis (Walter, 1983). Anoxygenic photosynthetic bacteria are known to use a wide variety of substrates as electron donors in photosynthesis, including hydrogen, sulfide, and small organic molecules (e.g. short-chain fatty acids). The capacity to grow by anoxygenic photosynthesis is even known in some cyanobacteria (Cohen *et al.*, 1975; Padan, 1979; Rye & Nealson, 2004). Thus, even if we accept the morphological fossil evidence for the Archean cyanobacteria (Schopf, 1993; Kazmierczak & Altermann, 2002), and the geochemical biomarker evidence (Brocks *et al.*, 1999), we cannot argue that these ancient organisms actually evolved oxygen.

Towards the goal of building experimental models of stromatolite growth for a variety of microorganisms, we set out to test whether anoxygenic photosynthetic bacteria could influence the precipitation of carbonate minerals and stabilize sediment grains under conditions relevant for ancient oceans. To our knowledge, this idea has not been tested experimentally. Specifically, we considered whether an anoxygenic photosynthetic α-proteobacterium, *Rhodopseudomonas palustris* (further referred to as *R. palustris*) (Harwood & Gibson, 1988), could influence *in situ* calcite precipitation and the formation of calcium carbonate crusts in solutions containing high concentrations of dissolved inorganic carbon (DIC). Although purple nonsulfur bacteria usually do not form strata in modern microbial mats, they are a tractable laboratory substitute for purple sulfur bacteria that typically form layers in microbial mats. Purple nonsulfur bacteria may also play a previously underappreciated role in some natural microbialites, particularly the microbial community associated with modern hypersaline stromatolites in Shark Bay (Papineau *et al.*, 2005).

MATERIALS AND METHODS

Growth medium

We grew *R. palustris* strain CGA009 (provided by C. Harwood) on hydrogen in the presence of 0.2 mM $Na_2S_2O_3$ in modified, bicarbonate-buffered photosynthetic medium at 25 °C. The basal medium contained: 0.3 g L^{-1} $(NH_4)_2SO_4$, 0.1 mM KH_2PO_4, 0.9 g L^{-1} KCl, 0.4 g L^{-1} $MgCl_2$,0.1 mM $Na_2S_2O_3$, 1 mL L^{-1} of 1 g L^{-1} PABA, and 1 mL L^{-1} concentrated base. The concentrated base contained 20 g L^{-1} nitriloacetic acid, 28.9 g L^{-1} anhydrous $MgSO_4$, 6.67 g L^{-1} $CaCl_2 \cdot 2H_20$, 18.5 mg L^{-1} $(NH_4)_6Mo_7O_{24} \cdot 4H_20$, 198 mg L^{-1} $FeSO_4 \cdot 7H_2O$ and 100 mL L^{-1} of Metal 44 solution. Metal 44 solution contained 2.5 g EDTA, 10.95 g $ZnSO_4 \cdot 7H_2O$, 5 g $FeSO_4 \cdot 7H_20$, 1.54 g $MnSO_4 \cdot H_20$, 392 mg $CuSO_4 \cdot 5H_20$, 250 mg $Co(NO_3)_2 \cdot 6H_2O$, and 177 mg $Na_2B_4O_7 \cdot 10H_2O$ per 800 mL. The medium was boiled under nitrogen, cooled under a mixed atmosphere of 80% N_2 and 20% CO_2, amended with 40 mL of 1 M $NaHCO_3$ from sterile stock solution, and left to equilibrate with an atmosphere of 80% N_2, 15% CO_2 and 5% H_2 (adding to 1 atmosphere total) for at least one day. The pH was adjusted by 10 N NaOH to 7.4–7.5, and the medium was filter-sterilized by a 0.2-μm filter and stored in the anaerobic glove box for at least a week before it was used in the experiments. All the glassware used in the experiments were stored in the anaerobic glove box for at least a week before they were used in experiments.

Growth conditions

An incandescent light bulb (75 W) served as the light source. Different light intensities were obtained by moving the cultures toward or away from the light (making sure that the temperature was constant). The light intensities were measured by a dual-range lightmeter (Traceable® by Control Company, Friendswood, TX, USA). Growth at 3.8 μmol photon $\cdot m^{-2} \cdot s^{-1}$ was measured by daily cell counts of DAPI-stained cells from triplicate tubes. The growth rate at 7.8 μmol photon $\cdot^{-2} \cdot s^{-1}$ was not measured, but we noted that the same optical densities at this light intensity were reached in considerably shorter time. All culturing and

precipitation experiments were performed in the anaerobic glove box under an atmosphere of 80% N_2, 15% CO_2, and 5% H_2. These chemical conditions are within the large limits of uncertainty of the chemical composition of the Archean oceans (Kempe & Degens, 1985; Grotzinger & Kasting, 1993), and are consistent with the inferred low sulfate concentration (Habicht *et al.*, 2002), higher pCO_2 (Kaufman & Xiao, 2003) and very low atmospheric oxygen content (Farquhar *et al.*, 2000). We conducted all experiments at a temperature that was lower than the standard temperature used to enrich and isolate purple nonsulfur bacteria (30 °C) for technical reasons. Due to decreased solubility of calcium carbonate at higher temperatures, we expect *R. palustris* to stimulate the precipitation of minerals at lower concentrations of calcium and protons when grown at 30 °C.

Precipitation experiments

Mid-exponential phase cells (10^8 cells mL^{-1}) were centrifuged to remove the liquid phase. The cells were resuspended into 2.5 mL of the sterile culture medium in triplicate screw-capped glass tubes to cell densities of 1.4×10^8 and 1.4×10^9 cells mL^{-1} (the latter corresponding to early stationary phase cell density). To distinguish between the influence of actively photosynthesizing cells and the influence of inactive cellular material on calcite precipitation, we inoculated triplicate glass tubes to a cell density of 1.4×10^8 cells mL^{-1} and covered them with aluminium foil. Three tubes with 2.5 mL of sterile culture medium were incubated without any cells as abiotic controls. After inoculation, 1 M $CaCl_2$ was added to all tubes to 12 mM final concentration. The tubes were incubated at 25 °C at light intensities of 3.8 and 7.8μmol photon $\cdot m^{-2} \cdot s^{-1}$, respectively, and with a 12-h day, 12-h night cycle regulated by a timer. Every 2 days, we took 120 μL samples, filtered them, and added 100 μL of the filtrate to 10 mL of 1% HNO_3. We monitored the pH of the cultures in the absence of calcium ions and minerals, because the generation of protons during precipitation of calcium carbonate would have balanced any metabolically driven increase of the pH. We measured the calcium concentration in these samples by inductively coupled plasma mass spectrometry (ICP-MS) at the Environmental Analysis Facility at Caltech. The crystals were collected by a sterile pipette, visualized by light microscopy and point counted. To point count the precipitated crystals, we conducted parallel experiments in 8-well LabTek® (Nalge Nunc International, Rochester, NY, USA) chambered coverglass culture dishes with coverslip bottoms. The crystal structure of the precipitates was determined by X-ray diffraction using a Scintag diffractometer with Cu Kα (λ = 1.5405Å).

Precipitation in the reactors

Figure 1 depicts our experimental setup. Thirty millilitres of the sterile culture medium was added to each of the two ~40 mL working volume sterile glass reactors containing 12 sterile plastic chips, and left to equilibrate in the anaerobic chamber for a week. Five millilitres of mid-exponential *R. palustris* culture was then added to each reactor; the cells were incubated for a week with a 12-h light, 12-h dark cycle at 3.8 and 7.8 μmol photon$\cdot m^{-2} \cdot s^{-1}$, respectively. We replaced the culture medium weekly with a 1:1 mixture of the Ca- and bicarbonate-containing sterile media. The culture medium was not additionally inoculated during exchange, but was repopulated by the growth of the surface-attached cells that remained in the reactors. The alkalinity of the experimental solutions was determined by Gran-titration of 10-mL samples using 0.8 M H_2SO_4. Plastic chips covered by biofilms and precipitates were removed weekly from each reactor, and were fixed in Karnovsky fixative after collection (Glauert, 1975). Confocal images of Dead/Live BacLight©-stained biofilms (Invitrogen Corp., Carlsbad, CA, USA) were taken weekly by a Zeiss LSM Pascal inverted confocal microscope. The excitation wavelength was 488 nm. The green BP505–540 and the red LP580 bands were separated by a 545 nm dichroic mirror. The images were analysed by Zeiss LSM software (Carl Zeiss Microimaging Inc., Thornwood, NY, USA).

SEM Imaging

The plastic chips were rinsed several times with cacodylate buffer (0.2 M, pH 7.5), post-fixed with 1% OsO_4 in water for 6 h, rinsed again several times in cacodylate buffer, dehydrated in a graded series of ethanol (30%, 50%, 70%, 90%, and 100%), and progressively infiltrated with LR White resin (EMS, Hartfield, PA, USA) for 6 h prior to polymerization at 65 °C for 24 h. The crystals visible under the light microscope prior to the rinsing remained on the chips after the treatment, indicating that they did not dissolve appreciably during the rinsing procedure. After the polymerization, a transverse section was polished (Wierzchos & Ascaso, 1994), carbon coated and imaged by a LEO 1550 VP SEM (Carl Zeiss SMT, Thornwood, NY, USA) equipped with an energy-dispersive X-ray spectrophotometer (EDS) using the backscattered-electron detector operating at 15 kV and a working distance of 10 mm.

RESULTS

Stimulation of $CaCO_3$ precipitation in active photosynthetic cultures

Anoxygenic photosynthetic bacteria use various inorganic and organic compounds as electron donors to inorganic carbon. Many of these compounds, such as iron(II), reduced sulfur compounds, and molecular hydrogen, could have been present on an anoxic early Earth before the rise of oxygen.

Eqs 1–3 describe photosynthetic growth with molecular hydrogen as an electron donor:

$$2H_2 \rightarrow 4H^+ + 4c^- \quad \text{(Eq. 1)}$$

$$HCO_3^- + 4c^- + 5H^+ \rightarrow CH_2O + 2H_2O \quad \text{(Eq. 2)}$$

$$2H_2 + HCO_3^- + H^+ \rightarrow CH_2O + 2H_2O \quad \text{(Eq. 3)}$$

The uptake of protons increases the pH and shifts the carbonate equilibrium toward an increase in the concentration of carbonate ions:

$$HCO_3^- \rightarrow CO_3^{2-} + H^+ \quad \text{(Eq. 4)}$$

The saturation index (SI) of calcite increases, driving the precipitation of calcite (Eqs 5–6)

$$SI = \log \frac{\{Ca^{2+}\}\{CO_3^{2-}\}}{K_s} \quad \text{(Eq. 5)}$$

$$Ca^{2+} + CO_3^{2-} \rightarrow CaCO_3 \quad \text{(Eq. 6)}$$

K_s is the solubility constant of calcite (see Methods) {} denote the activities of specific ions.

The growth of anoxygenic phototrophs on hydrogen as described by Eq. 1 and Eq. 2 results in the same net production of carbonate ions as oxygenic photosynthesis, and would be predicted

to have the same net effect on the precipitation of calcium carbonate per mole of electron donor. The effect would be expected to be negligible if the solution were buffered by a large amount of bicarbonate because photosynthesis could not appreciably increase the pH.

Given that the culture medium in our experiments was well buffered (alkalinity 51.9 ± 0.2 meq L^{-1}) and in equilibrium with a large reservoir of CO_2, we were surprised to find that both the number of visible individual crystals and the total amount of precipitate relative to sterile controls were higher in the presence of *R. palustris* cells (Fig. 2A). To elucidate whether it was an active metabolism or just the presence of cell surfaces that stimulated calcite nucleation relative to sterile controls (Bosak & Newman, 2003,2005), we incubated *R. palustris* cells at two different cell densities, two different light intensities (and, consequently, two different growth rates), and in the presence and absence of light (Fig. 2A). We found that the removal of calcium at the same cell density started earlier and proceeded faster at 7.8 μmol photon·$m^{-2} \cdot s^{-1}$ than at 3.8 μmol photon·$m^{-2} \cdot s^{-1}$, or in the dark cultures, respectively (Fig. 2A). The crystals in the light cultures (Fig. 2B) were more numerous, larger, and less acicular than the crystals in the dark cultures (not shown) and were covered by attached *R. palustris* cells (Fig. 2C). Thus, the light-dependent metabolic activity of *R. palustris* both stimulated calcite precipitation and influenced crystal morphology.

Active anoxygenic photosynthesis and the precipitation of calcite crusts

Photosynthetic stimulation of calcite precipitation by active *R. palustris* cells posed the following question: would temporal variations in the biomass and the cell activity affect the growth of calcite crusts, and, by extension, stromatolite lamina? We explored how anoxygenic photosynthetic growth of micron-sized, nonfilamentous microbes translates into the textures of accreting $CaCO_3$ crusts in a more than 1-month-long precipitation experiment in bioreactors (Fig 1,Fig 3,Fig 4).

Rhodopseudomonas palustris cells in the first reactor grew at 7.8 μmol photon·$m^{-2} \cdot s^{-1}$ in the absence of Ca for 1 week. The medium was then replaced by Ca-containing medium, and the reactor was incubated at 7.8 μmol photon·$m^{-2} \cdot s^{-1}$ for 2 weeks with a stir bar used to maintain a thoroughly mixed culture (Fig. 3). Although the alkalinity of the reactor solution dropped over time, this was due to the precipitation of calcite, not a metabolic pH effect *per se* (i.e. the alkalinity remained constant in control cultures that contained no calcium) (Fig. 3A). Cell growth stimulated the precipitation of visible low-Mg calcite crusts that become more compact and thicker over time (Fig. 3B,C,G). Meanwhile, there was no precipitation in the sterile culture medium (i.e. in the absence of cells or seed crystals). Moreover, there was no observable precipitation in the second reactor where the cells had grown for 2 weeks at 3.8 μmol photon·$m^{-2} \cdot s^{-1}$ before the addition of calcium (Fig. 4A,B) and the crusts only formed in the second reactor when the cells started growing at 7.8 μmol photon·$m^{-2} \cdot s^{-1}$ (Fig. 4C,D). When the first reactor with a dense population of cells was covered with aluminium foil, photosynthetic growth ceased, cells and their density decreased, and both the biofilms and the crusts disappeared (Fig. 3A.D). The cell density declined and the crusts similarly disappeared in the second reactor when we covered it by aluminium foil (Fig. 4E). The calcite from the crusts was ground up by the stir bar into micron-sized suspended grains that clouded the solution. The decrease in alkalinity in the dark was 5.0 ± 1.5 meq L^{-1} smaller than that at 7.8 μmol photon·$m^{-2} \cdot s^{-1}$, suggesting that less mineral precipitation was taking place in the absence of light. When we removed the foil from the first reactor, the cells grew at 7.8 μmol photon·$m^{-2} \cdot s^{-1}$ to 1.1×10^8 cells mL^{-1}, the solution remained cloudy with small crystals, and biofilms and small calcite crystals reappeared on the plastic chips (Fig. 3E,F). The crystal grain size differed in the presence or absence of suspended sediment; long (>15 μm) crystals were observed in the absence of abundant nuclei (Fig 3B,C,G, Fig 4C,D), as opposed to the smaller (<5 μm) crystals observed around abundant nuclei (Fig. 3E,F,H). The biofilms grew around

the large and small crystal grains, stabilizing the grains into crusts (Fig. 3G,H,I). Although the cultures grew with 12 h of light and 12 h of darkness, there were no obvious alternating morphological features in the crusts that would correspond to this daily light cycle.

DISCUSSION

Our calculations and experiments required that the pH increase by at least 0.5 pH units for calcite to precipitate in the sterile growth medium, but *R. palustris* actively stimulated calcite precipitation in the absence of measurable pH (and SI) changes in the growth medium. The pH and the SI might have increased only locally, within diffusion-limited ~30 μm biofilms, but we consider large gradients between the liquid medium and the biofilms unlikely because the liquid medium itself contained more than 10^8 cells mL^{-1}. In addition, field observations and chemical modelling results imply that the photosynthetic uptake of CO_2 in well-buffered high-DIC solutions is not likely to induce the precipitation of calcium carbonate (Merz-Preiss & Riding, 1999; Arp *et al.*, 2001), although there are reports of carbonate-encrusted cyanobacteria-like microbes that formed in presumably well-buffered Archean seas (Kazmierczak & Altermann, 2002). Metabolically active cells might have stimulate calcite precipitation kinetically, either by secreting extracellular compounds into the medium or by taking up metabolites that kinetically inhibit calcite nucleation and precipitation (e.g. phosphate, trace metals, or organic compounds during mixotrophic growth in the dark) (Braissant *et al.*, 2003; Dupraz *et al.*, 2004; Bosak & Newman, 2005; Gautret *et al.*, 2006). Such kinetic stimulation of calcium carbonate precipitation would be consistent with the proposed kinetic control of calcium carbonate precipitation in the Archean oceans (Sumner & Grotzinger, 1996). The stimulation of mineral precipitation by purple nonsulfur bacteria under our experimental conditions contrasts the observations from modern lithifying microbial mats. There, lithification seems to be inhibited by EPS in the photosynthetic layers and is primarily attributed to heterotrophic degradation of EPS (Dupraz *et al.*, 2004; Dupraz & Visscher, 2005). In our cultures exposed to light, where we would expect abundant EPS, precipitation actually starts at least 2 days earlier. This suggests a negligible inhibitory role for EPS under these conditions, but given the many possible chemical differences between EPS produced by different organisms, these results may be specific to our model organism.

Layers of many ancient stromatolites strongly selected for micritic calcium carbonate even when they grew in siliciclastic settings (e.g. Serebryakov & Semikhatov, 1974). A preference for micritic calcite despite siliciclastic settings is presumed to indicate microbial activity, but it is unclear whether microbes selected the sediment by trapping-and-binding, or by actively promoting cementation (Grotzinger, 1990; Fairchild, 1991). We find that not only does anoxygenic photosynthesis by *R. palustris* greatly stimulate calcite precipitation in the absence of initial inorganic nuclei, but it also traps crystals and enhances cementation even in the presence of abundant crystal nuclei. Grains larger than 20 μm stabilized by *R. palustris* imply that small anoxygenic photosynthetic microbes could have trapped and bound grains of similar size in the ancient stromatolites. The change of crystal grain size during the course of our experiment in a medium of constant chemical and biological composition shows that mechanisms other than community composition and the size of trapping-and-binding microbes can control the grain size in many stromatolites (Awramik & Semikhatov, 1979; Awramik & Riding, 1988). In our experiments, the dominant factor that determines the size of the crystals in the crusts seems to be the number of available crystal nuclei (Bosak *et al.*, 2004). Active photosynthetic microbes would have thus strongly promoted the growth of ancient stromatolites by both accumulating the sediment and stimulating *in situ* precipitation even in highly saturated solutions.

Because enhanced cementation in itself is a poor biomarker, a productive avenue for future studies might be to focus on the textural and chemical signatures in experimental cemented

structures that could be used to understand putative microbial biosignatures in ancient structures. A particularly interesting avenue of investigation would be to compare and contrast any signatures in the precipitates formed in the presence of anaerobic and anoxygenic communities as opposed to cyano-bacterially driven communities. In the late Archean and Palaeoproterozoic, local conditions could have favoured microbial communities driven by either anoxygenic or oxygenic photosynthesis and could have resulted in different types of microbial laminites. A good example of unusual laminites that may have precipitated in the presence of anoxygenic and anaerobic communities are those formed below storm-wave base as described by Simonson *et al.* (1993) and Sumner (1997a, b).

Overall, our experiments support the interpretation of ancient stromatolites as 'carbonate factories' -structures that relied on extensive carbonate precipitation in addition to trapping-and-binding (Grotzinger, 1990; Grotzinger & Knoll, 1999) and show that anoxygenic photosynthetic bacteria could have promoted their growth. In the future, we plan to use mixed communities (with and without cyanobacteria) to investigate lithification processes that would have taken place before the evolution of oxygenic photosynthesis.

CONCLUSIONS

Although anoxygenic photosynthesis does not dominate primary production in modern stromatolites, this metabolism may have been crucial for the growth of Archean and some Palaeoproterozoic stromatolites. Light-dependent activity of micron-sized, nonfilamentous anoxygenic photosynthetic organisms can increase the amount of $CaCO_3$, facilitate the accretion of lamina and stabilize accreting surfaces against mechanical damage. In contrast to the predictions of equilibrium chemical models, photosynthetic activity in high-DIC solutions can significantly stimulate $CaCO_3$ nucleation even when the cells are unable to significantly increase the pH or the SI of the bulk medium. The crystal grain size in the high-DIC growth medium depends chiefly on the number of nuclei for crystal growth even when the microbes associated with the accreting crusts, or the chemical parameters, do not vary. When the nuclei are limited, photosynthetic activity may be essential to remove kinetic inhibition of the crystal nucleation. Even when micritic nuclei are abundant, the binding and the stabilization of the carbonate crusts rely on active photosynthetic biofilms, promoting rapid growth of carbonate structures in highly saturated solutions. Thus, biofilms formed by anoxygenic photosynthetic microorganisms would have helped build stromatolites even before cyanobacteria became the dominant primary producers in Precambrian reefs.

Acknowledgments

We thank the Agouron Institute, Packard Foundation, and Howard Hughes Medical Institute for financial support and our reviewers for their helpful comments.

REFERENCES

Allwood A, Walter M, Kamber B, Marshall C, Burch I. Stromatolite reef from the Early Archaean era of Australia. Nature 2006;441:714–718. [PubMed: 16760969]

Altermann W, Kazmierczak J, Oren A, Wright D. Cyanobacterial calcification and its rock-building potential during 3.5 billion years of Earth history. Geobiology 2006;4:147–166.

Arp G, Reimer A, Reitner J. Photosynthesis-induced biofilm calcification and calcium concentrations in phanerozoic oceans. Science 2001;292:1701–1704. [PubMed: 11387471]

Awramik SM, Riding R. Role of algal eukaryotes in subtidal columnar stromatolite formation. Proceedings of the National Academy of Sciences of the USA 1988;85:1327–1329. [PubMed: 16593910]

Awramik SM, Semikhatov MA. Relationship between morphology, microstructure, and microbiota in 3 vertically intergrading stromatolites from the gunflint iron formation. Canadian Journal of Earth Sciences 1979;16:484–495.

Bosak T, Newman DK. Microbial nucleation of calcium carbonate in the Precambrian. Geology 2003;31:577–580.

Bosak T, Newman DK. Microbial kinetic controls on calcite morphology in supersaturated solutions. Journal of Sedimentary Petrology 2005;75:190–199.

Bosak T, Souza-Egipsy V, Newman DK. A laboratory model of abiotic peloid formation. Geobiology, 2004:189–198.

Braissant O, Cailleau G, Dupraz C, Verrecchia AP. Bacterially induced mineralization of calcium carbonate in terrestrial environments: The role of exopolysaccharides and amino acids. Journal of Sedimentary Research 2003;73:485–490.

Brocks JJ, Logan GA, Buick R, Summons RE. Archean molecular fossils and the early rise of eukaryotes. Science 1999;285:1033–1036. [PubMed: 10446042]

Buick R, Dunlop JSR, Groves DI. Stromatolite recognition in ancient rocks - an appraisal of irregularly laminated structures in an Early Archean Chert-Baritc Unit from North-Pole, Western-Australia. Alcheringa 1981;5:161–181.

Buick R, Groves DI, Dunlop JSR. Abiological origin of described stromatolites older than 3.2 Ga - comment. Geology 1995;23:191. [PubMed: 11540143]

Cohen Y, Jorgensen B, Padan E, Shilo M. Sulphide-dependent anoxygenic photosynthesis in cyanobacterium Oscillatoria limnetica. Nature 1975;257:489–492.

Dietrich L, Tice M, Newman D. The co-evolution of life and Earth. Current Biology 2006;16:R395–R400. [PubMed: 16753547]

Dupraz C, Visscher PT. Microbial lithification in marine stromatolites and hypersaline mats. Trends in Microbiology 2005;l3:429–438. [PubMed: 16087339]

Dupraz C, Visscher PT, Baumgartner LK, Reid RP. Microbe-mineral interactions: early carbonate precipitation in a hypersaline lake (Eleuthera Island, Bahamas). Sedimentology 2004;51:745–765.

Fairchild IJ. Origins of carbonate in Neoprotcrozoic stromatolites and the identification of Modern Analogs. Precambrian Research 1991;53:281–299.

Farquhar J, Bao HM, Thiemens M. Atmospheric influence of Earth's earliest sulfur cycle. Science 2000;289:756–758. [PubMed: 10926533]

Gautret P, Wit D, Camoin G, Golubic S. Are environmental conditions recorded by the organic matrices associated with precipitated calcium carbonate in cyanobacterial microbialites? Geobiology 2006;4:93–107.

Glauert, AM. Fixation, dehydration and embedding of biological samples. In: Glauert, AM., editor. Practical Methods in Electron Microscopy. Amsterdam: Elsevier North-Holland Biomcdical Press; 1975. p. 48

Grotzinger JP. Gcochemical model for Protcrozoic stromatolite decline. American Journal of Science 1990;290A:80–103.

Grotzinger JP, Kasting JF. New constraints on Precambrian ocean composition. Journal of Geology 1993;101:235–243. [PubMed: 11537740]

Grotzinger JP, Knoll AH. Stromatolites in Precambrian carbonates: evolutionary mileposts or environmental dipsticks? Annual Review of Earth and Planetary Sciences 1999;27:313–358.

Grotzinger JP, Rothman DH. An abiotic model for stromatolite morphogenesis. Nature 1996;383:423–425.

Habicht KS, Gade M, Thamdrup B, Berg P, Canfield DE. Calibration of sulfate levels in the Archean Ocean. Science 2002;298:2372–2374. [PubMed: 12493910]

Harwood CS, Gibson J. Anacrobic and Aerobic metabolism of diverse aromatic-compounds by the photosynthetic bacterium *Rhodopseudomonas palustris*. Applied and Environmental Microbiology 1988;54:712–717. [PubMed: 3377491]

Hoffman HJGK, Hickman AH, Thorpe RI. Origin of 3.45 Ga coniform stromatolites in Warrawoona Group, Western Australia. Geological Society of America Bulletin 1999;111:1256–1262.

Kaufman AJ, Xiao SH. High CO_2 levels in the Proterozoic atmosphere estimated from analyses of individual microfossils. Nature 2003;425:279–282. [PubMed: 13679912]

Kazmierczak J, Altermann W. Neoarchean biomineralization by benthic cyanobacteria. Science 2002;298:2351. [PubMed: 12493906]

Kazmierczak J, Kempe S. Genuine modern analogues of Precambrian stromatolites from caldera lakes of Niuafo'ou Island, Tonga. Naturwissenschaften 2006;94:119–126. [PubMed: 16365738]

Kempe S, Degens ET. An early soda ocean? Chemical Geology 1985;53:96–108.

Lowe DR. Abiological origin of described stromatolites older than 3.2 Ga. Geology 1994;22:387–390. [PubMed: 11540142]

Merz-Preiss M, Riding R. Cyanobacterial tufa calcification in two freshwater streams: ambient environment, chemical thresholds and biological processes. Sedimentary Geology 1999;126:103–124.

Olson JM, Blankenship RE. Thinking about the evolution of photosynthesis. Photosynthesis Research 2004;80:373–386. [PubMed: 16328834]

Padan E. Facultative anoxygenic photosynthesis in cyanobacteria. Annual Review of Plant Physiology and Plant Molecular Biology 1979;30:27–40.

Papineau D, Walker JJ, Mojzsis SJ, Pace NR. Composition and structure of microbial communities from stromatolites of Hamelin Pool in Shark Bay, Western Australia. Applied and Environmental Microbiology 2005;71:4822–4832. [PubMed: 16085880]

Reid RP, Visscher PT, Decho AW, Stolz JF, Bebout BM, Dupraz C, Macintyre LG, Paerl HW, Pinckney JL, Prufert-Bebout L, Steppe TF, DesMarais DJ. The role of microbes in accretion, lamination and early lithification of modern marine stromatolites. Nature 2000;406:989–992. [PubMed: 10984051]

Riding R, Awramik SM, Winsborough BM, Griffin KM, Dill RF. Bahamian giant stromatolites - microbial composition of surface mats. Geological Magazine 1991;128:227–234.

Rye, R.; Nealson, KH. Evolution of metabolism. In: Schlesinger, WH., editor. Biogeochemistry. Oxford: Elsevier-Pergamon; 2004. p. 41-62.

Schopf JW. Microfossils of the early Archean Apex chert: new evidence of the antiquity of life. Science 1993;260:640–646. [PubMed: 11539831]

Semikhatov MA, Gebelein CD, Cloud P, Awramik SM, Benmore WC. Stromatolite morphogenesis - progress and problems. Canadian Journal of Earth Sciences 1979;16:992–1015.

Serebryakov SN, Semikhatov MA. Riphean and Recent stromatolites: a comparison. American Journal of Science 1974;274:556–574.

Simonson BM, Schubel KA, Hassler SW. Carbonate sedimentology of the early Precambrian Hamersley Group of Western Australia. Precambrian Research 1993;60:287–335.

Sumner DY. Late Archean calcite-microbe interactions: two morphologically distinct microbial communities that affected calcite nucleation differently. PALAIOS 1997a;12:302–318.

Sumner DY. Carbonate precipitation and oxygen stratification in late Archean seawater as deduced from facies and stratigraphy of the Gamohaan and Frisco formations, Transvaal Supergroup, South Africa. American Journal of Science 1997b;297:455–487.

Sumner DY, Grotzinger JP. Were kinetics of Archean calcium carbonate precipitation related to oxygen concentration? Geology 1996;24:119–122. [PubMed: 11539494]

Walter, MR. Archean stromatolites: evidence of the Earth's earliest benthos. In: Schopf, JW., editor. The Earth's Earliest Biosphere: Its Origin and Evolution. Princeton, NJ: Princeton University Press; 1983. p. 187-213.

Walter MR, Buick R, Dunlop JSR. Stromatolites 3400–3500 Myr old from the North-Pole Area, Western-Australia. Nature 1980;284:443–445.

Wierzchos J, Ascaso C. Application of back-scattered electron imaging to the study of the lichen-rock interface. Journal of Microscopy 1994;175:54–59.

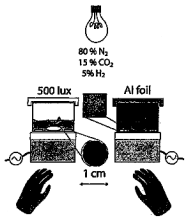

Fig. 1.

Setup for the long-term precipitation experiments. The biofilms were grown photosynthetically in an anaerobic hood. Two 9-cm diameter glass reactors were covered with removable glass lids and multiple 1-cm diameter polycarbonate chips provided a submerged growth surface for carbonate crusts and biofilms. Every week, the growth medium was replaced and sample chips were removed from each of the reactors with ethanol-sterilized tweezers. The light conditions were varied either by changing the distance between the reactors and the light source, or by wrapping the entire reactor in aluminium foil (dark). Magnetic stir bars ensured the constant stirring of the growth medium. Calcium carbonate crusts only accreted on the chips in the presence of well-developed biofilms (as shown by the photographs of the chips from the light and dark conditions in the diagram).

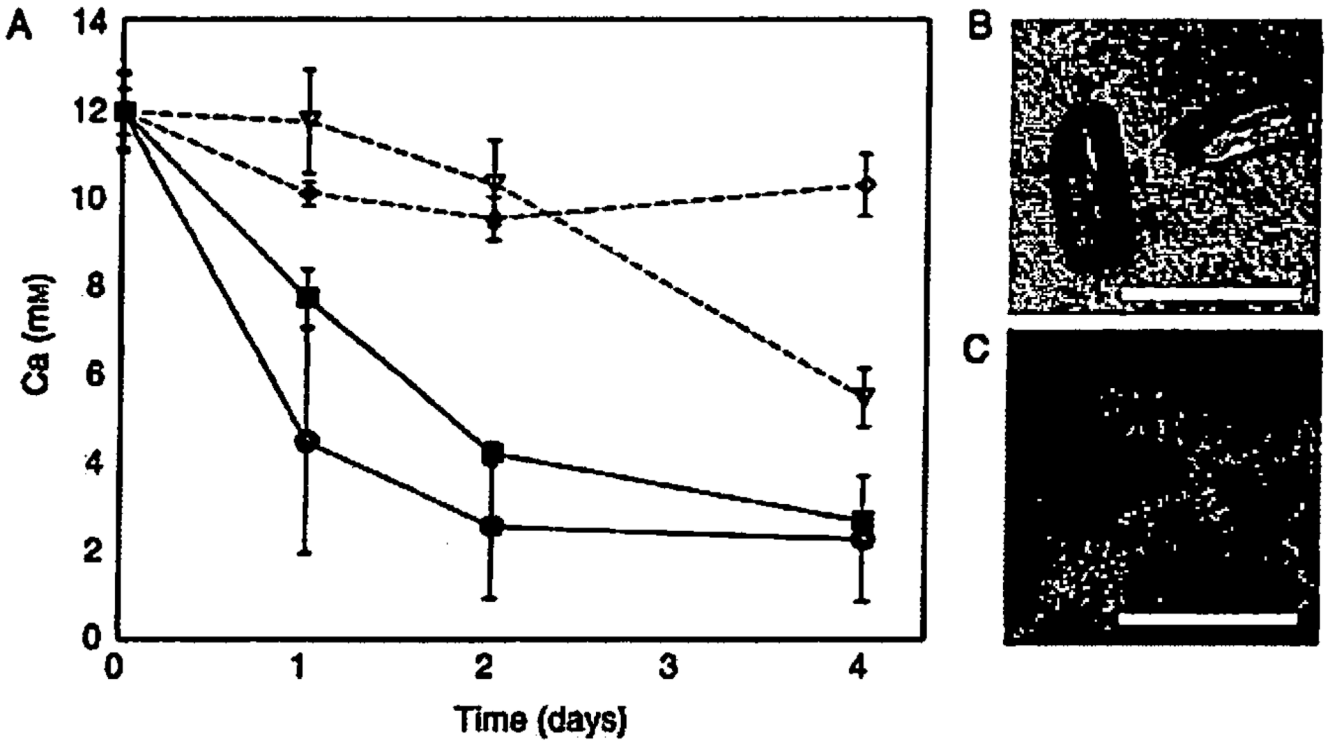

Fig. 2.

Removal of calcium from the photosynthetic growth medium stimulated by the photosynthetic activity of *Rhodopseudomonas palustris*. (A) Total calcium was measured by ICP-MS in triplicate samples. Black circles: an initial inoculum of 10^8 cells mL^{-1} at 7.8 μmol photon·$m^{-2} \cdot s^{-1}$. Black squares: an initial inoculum of 10^8 cells mL^{-1} at 3.8 μmol photon·$m^{-2} \cdot s^{-1}$. Empty triangles: an initial inoculum of 10^8 cells mL^{-1} wrapped in Al-foil. Empty diamonds: sterile control solution kept at the same distance from the light as the black circle samples, *y*-axis shows the concentration of calcium (mM) in the medium. Although the calcium concentration decreased in sterile controls, we did not detect any mineral precipitates either by light microscopy or XRD. (B) Transmitted-light micrograph of calcite crystals that grew in the presence of photosynthetica1ly active cells. (C) Top-view confocal micrograph of the epifluorescently stained cells (green/yellow) growing on crystals (red). The scale bar in B and C is 15 μm.

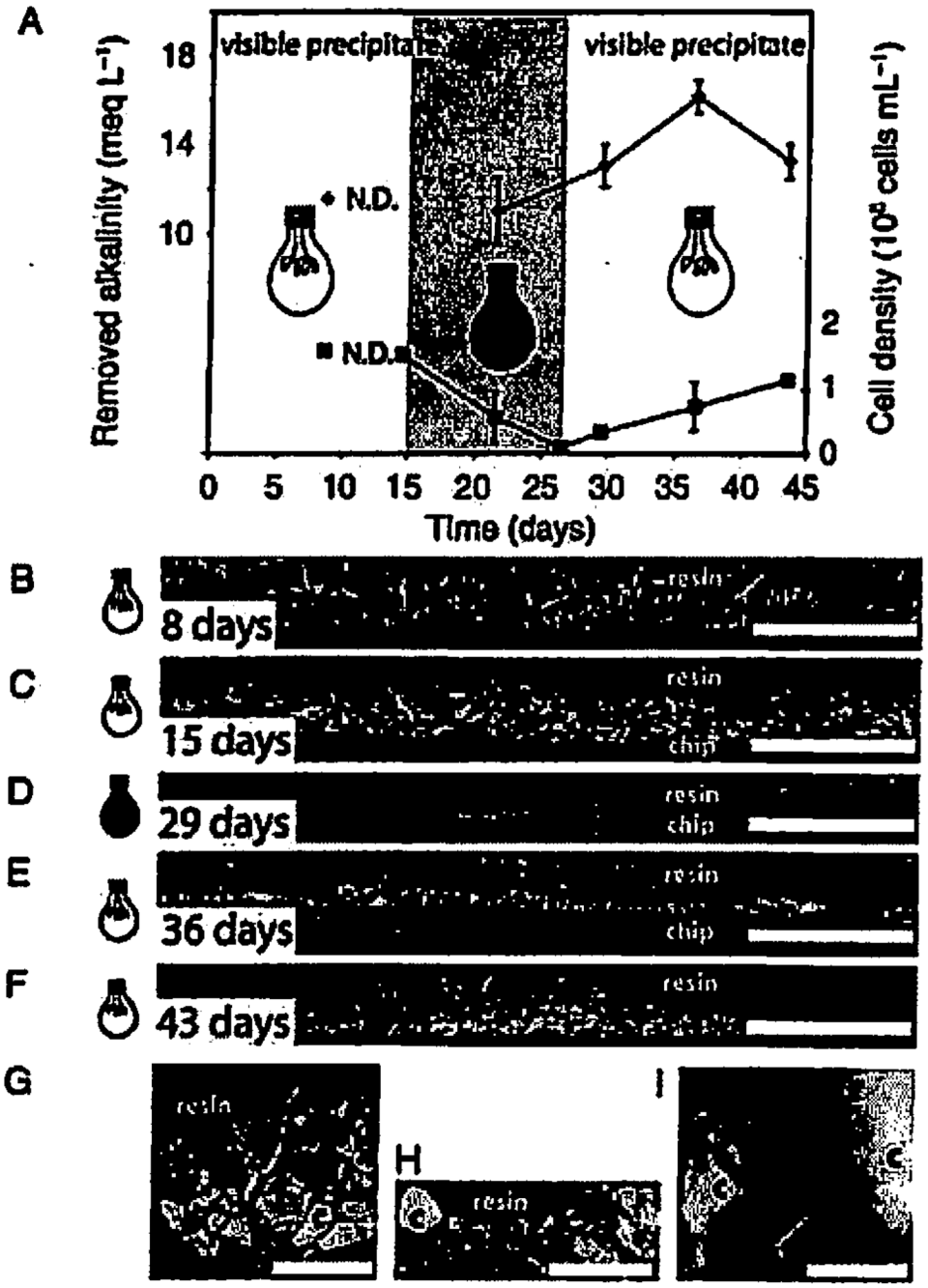

Fig. 3.

Alkalinity, cell density and scanning electron micrographs (SEM) of the polished vertical cross-sections of calcite crusts as a function of the light conditions in the first reactor. (A) Diamonds and left *y*-axis: decrease in alkalinity in meq L^{-1} (measured relative to the sterile control solution). Squares and right *y*-axis: cell density (measured by microscopic counting of epifluorescently stained cells). (B, C) *Rhodopseudomonas palustris* biofilms were grown for 2 weeks at 7.8 μmol photon·$m^{-2} \cdot s^{-1}$ (white light bulb) and calcium was then added to the biofilms. B shows the thickness of the calcite crusts (light grey) 8 days after the addition of calcium and C after 16 days. (D) 16 days after the addition of calcium, the reactor was completely covered with aluminium foil (black light bulb). The calcite crusts and the biofilm

have disappeared, and all that can be seen is the interface between the chip and the resin. After this, the foil was removed on the 29th day since the addition of calcium. (E, F) Emerging biofilms and small calcite crystals (lightest grey) 1 week (E) and 2 weeks (F) after the foil was removed. (G) Large crystals (c, light grey) formed during the first 2 weeks in the presence of biofilms (b, medium grey). (H) A close-up of the sparser and smaller crystals (c) and re-established biofilms (b) after the removal of the foil. (I) A close-up of the biofilms (b) surrounding the crystals (c). The arrow is pointing to a cross-section of a cell. The scale bar is 100 μm in A–F, 30 μm in G, 15 μm in H, and 2 μm in I, respectively.

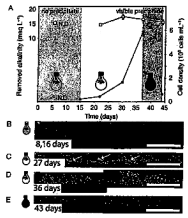

Fig. 4.

Alkalinity, cell density and scanning electron micrographs (SEM) of the polished vertical cross-sections of calcite crusts as a function of the light conditions in the second reactor. (A) Removed alkalinity (squares and the left *y*-axis) from the medium and the cell density (circles and the right *y*-axis) in the solution. The cells in the second reactor grew at lower light intensity (3.8 μmol photon·$m^{-1} \cdot s^{-1}$) for 2 weeks before the addition of calcium and formed only a sparse monolayer on the surface of the plastic chips. (B) During the first 2 weeks after the addition of calcium, there were no visually detectable mineral precipitates as shown by this representative SEM image of the vertical cross-section of the plastic chip covered by the resin. (C, D) Calcite crusts covered by biofilms formed when the cells were grown at 7.8 μmol photon·$m^{-2} \cdot s^{-1}$. The white arrows point to individual crystals. (E) Only sparse monolayers of cells and very few crystals remained on the surface of the plastic chips when we covered the dense culture in the reactor with aluminium foil 36 days after the beginning of the experiment. Although alkalinity was removed in the dark, there was no detectable crust formation in the absence of photosynthetic biofilms. The scale bar in B–F is 100 μm.